

**Biodistribution and immuno-PET imaging  
analysis of  $^{68}\text{Ga}$ -NOTA-Cetuximab Fab in an  
EGFR over-expressing cancer xenograft model**

**Do Wan Kim**

**The Graduate School  
Yonsei University  
Department of Biomedical Laboratory Science**

**Biodistribution and immuno-PET imaging  
analysis of  $^{68}\text{Ga}$ -NOTA-Cetuximab Fab in an  
EGFR over-expressing cancer xenograft model**

A Master's Thesis

Submitted to the Department of Biomedical  
Laboratory Science and the Graduate School of  
Yonsei University

in partial fulfillment of the  
requirements for the degree of  
Master of Science in Medical Technology

**Do Wan Kim**

**December 2008**

**This certifies that the master's thesis of  
Do wan Kim is approved.**

---

Thesis Supervisor : Ok Doo Awh

---

Tae Ue Kim : Thesis Committee Member

---

Yong Serk Park : Thesis Committee Member

The Graduate School

Yonsei University

December 2008

# CONTENTS

LIST OF FIGURES .....	iii
LIST OF TABLES .....	iv
ABBREVIATION .....	v
ABSTRACT IN ENGLISH .....	vi
I. INTRODUCTION .....	1
II. MATERIALS AND METHODS .....	8
1. Cell line .....	8
2. Evaluation of EGFR expression in cancer cells .....	8
2.1. Reverse transcriptase-polymerase chain reaction .....	8
2.2. Western blotting .....	9
2.3. Immuno-cytochemistry .....	10
3. Tumor model .....	12
4. Preparation of Cetuximab Fab fragments .....	13
5. Preparation of the radiolabeled Cetuximab and Cetuximab Fab fragments .....	14
5.1. Radiolabeling of Cetuximab and Cetuximab Fab fragments with iodine-125 .....	14
5.2. NOTA conjugation to Cetuximab Fab fragments .....	15
5.3. Radiolabeling of NOTA-Cetuximab Fab fragments with Gallium-68 .....	15
5.4. <i>In vitro</i> stability test of <sup>68</sup> Ga-NOTA Cetuximab Fab fragments ..	16
6. <i>In vitro</i> cellular binding test .....	17
7. Biodistribution assay of <sup>68</sup> Ga-NOTA-Cetuximab Fab	

fragments and $^{125}\text{I}$ -Cetuximab Fab fragments in EGFR over-expressing cancer xenograft mice .....	18
8. Small animal PET imaging of $^{68}\text{Ga}$ -NOTA-Cetuximab Fab fragments in EGFR over-expressing cancer xenograft mice .....	19
III. RESULTS .....	20
1. Evaluation of EGFR expression in cancer cells .....	20
2. Fragmentation of Cetuximab Fab fragments .....	20
3. Radiolabeling of Cetuximab and Cetuximab Fab fragments with $^{125}\text{I}$ and $^{68}\text{Ga}$ .....	26
4. <i>In vitro</i> characterization of $^{68}\text{Ga}$ -NOTA-Cetuximab Fab fragments .....	26
4.1. Chemical stability of $^{68}\text{Ga}$ -NOTA-Cetuximab Fab fragments .....	26
4.2. Immunoreactivity of $^{68}\text{Ga}$ -NOTA-Cetuximab Fab fragments .....	29
5. Biodistribution of radiolabeled Cetuximab Fab fragments ..	31
5.1. Biodistribution of $^{125}\text{I}$ -Cetuximab Fab fragments .....	31
5.2. Biodistribution of $^{68}\text{Ga}$ -NOTA-Cetuximab Fab fragments ..	31
6. Immuno-PET imaging with $^{68}\text{Ga}$ -NOTA-Cetuximab Fab fragments in mice bearing EGFR over-expression cancer xenograft .....	37
IV. DISCUSSION .....	40
V. REFERENCE .....	43
ABSTRACT IN KOREAN .....	50

## LIST OF FIGURES

Fig. 1. Epidermal growth factor receptor (EGFR) signal transduction and mechanism of Cetuximab .....	3
Fig. 2. Analysis of EGFR expression in A549 and CT26 cells by RT-PCR ..	22
Fig. 3. Analysis of EGFR expression in A549 and CT26 cells by Western blotting .....	23
Fig. 4. Analysis of EGFR expression in A549 and CT26 cells by Immunocytochemical staining with Cetuximab .....	24
Fig. 5. Analysis of Cetuximab and Cetuximab Fab fragments SDS-PAGE .....	25
Fig. 6. Analysis of radiolabeling yield of $^{68}\text{Ga}$ -NOTA-Cetuximab Fab fragments by ITLC-SG .....	27
Fig. 7. <i>In vitro</i> chemical stability of $^{68}\text{Ga}$ -NOTA-Cetuximab Fab fragments .....	28
Fig. 8. Cellular binding addinities of the radiolabeled Cetuximab derivatives .....	30
Fig. 9. Biodistribution of $^{125}\text{I}$ -Cetuximab Fab fragments in mice .....	34
Fig. 10. Biodistribution of $^{68}\text{Ga}$ -NOTA-Cetuximab Fab fragments in mice ..	36
Fig. 11. Immuno-PET imaging of A549 tumor-bearing mice taken at 1 hr post injection of $^{68}\text{Ga}$ -NOTA-Cetuximab Fab fragments ..	38
Fig. 12. Immuno-PET imaging of A549 tumor-bearing mice taken at 3 hr post injection of $^{68}\text{Ga}$ -NOTA-Cetuximab Fab fragments ..	39

## LIST OF TABLES

Table 1. EGFR over-expressing rate of cancer .....	4
Table 2. Primer sequence information .....	11
Table 3. Biodistribution of <sup>125</sup> I-Cetuximab Fab fragments in mice .....	33
Table 4. Biodistribution of <sup>68</sup> Ga-NOTA-Cetuximab Fab fragments in mice .....	35

## ABBREVIATION

Cetuximab : Anti EGFR chimeric antibody

EDTA : Ethylenediaminetetraacetic acid

EGFR : Epidermal growth factor receptor

FITC : Fluorescein isothiocyanate

Ga : Gallium

ITLC-SG : Instant thin layer chromatography - silica gel

NOTA : 1,4,7-triazacyclononane-1,4,7-triacetic acid

% ID/g : Percentage injected dose per gram

PET : Positron Emission Tomography

SDS-PAGE : Sodium dodecyl sulfate-polyacrylamide gel electrophoresis

## ABSTRACT

### **Biodistribution and immuno-PET imaging analysis of $^{68}\text{Ga}$ -NOTA-Cetuximab Fab in an EGFR over-expressing cancer xenograft model**

The Cetuximab (C225, anti-EGFR mAb) is a 152 kDa molecule, which is a chimeric monoclonal antibody that specifically binds to the epidermal growth factor receptor (EGFR) with a high affinity. EGFR is a transmembrane protein, and stimulates the cell proliferation. Further more, EGFR is involved in the pathogenesis of many tumors. At present time, the importance of immuno-PET (Positron Emission Tomography) have enlarged in detection and diagnosis of cancer. Gallium-68 ( $^{68}\text{Ga}$ ,  $T_{1/2} = 67.6$  min) is useful a PET imaging tracer because it emits positron and it is easily obtained using  $^{68}\text{Germanium}/^{68}\text{Ga}$  generator. In this study, a radio-imaging agent targeted to EGFR over-expressing cancer cells was developed and evaluated by biodistribution and the immuno-PET in nude mice bearing cancer xenograft. The Cetuximab Fab fragments were produced by enzyme digestion and their purity was assessed by SDS-PAGE analysis. EGFR expression in A549 and CT26 cells

were confirmed by the RT-PCR analysis, Western blotting and immuno-cytochemistry. According to these analysis, A549 cells have mRNA transcripts of EGFR and highly express transmembrane proteins of EGFR. The immunoreactivity of 1,4,7-triazacyclononane-1,4,7-triacetic acid (NOTA) conjugated Cetuximab Fab fragments was examined by the in vitro cellular binding test and it was approximately 55% of whole Cetuximab at the same molar concentration. The NOTA bifunctional chelator was adopted to label  $^{68}\text{Ga}$  to Cetuximab Fab fragments. The radiolabeling yield of  $^{68}\text{Ga}$ -NOTA-Cetuximab Fab fragments was determined by instant thin layer chromatography (ITLC), and the yield was above 95%. The organ biodistribution and small animal PET image of  $^{68}\text{Ga}$ -NOTA-Cetuximab Fab fragments were acquired in EGFR over-expressing cancer xenografts, and the radiolabeled conjugates were highly accumulated in the liver, kidneys and tumor. In conclusion, the  $^{68}\text{Ga}$ -Cetuximab Fab fragments will be efficient, harmless, rapid and non-invasive method of diagnosis for the EGFR over-expressing cancer. Because the gallium-68 has a short half life, and the Fab fragments has fast blood clearance in a few hours. Therefore, the damage of radiation was less than other radio-isotopes, and  $^{68}\text{Ga}$ -NOTA-Cetuximab Fab fragments need an injection at once. According to the data, the  $^{68}\text{Ga}$ -NOTA-Cetuximab Fab fragments may be an effective imaging agent targeted to the EGFR over-expressing cancer.

---

Keywords : EGFR, Cetuximab,  $^{68}\text{Ga}$ , NOTA, Fab

## I. INTRODUCTION

The epidermal growth factor receptor (EGFR) is a transmembrane receptor tyrosine kinase stimulated by growth factors, such as transforming growth factor (TGF)- $\alpha$  and epidermal growth factor (EGF), that bind to the extracellular domain of the receptor (Fig. 1-a) [1]. Ligand binding induces receptors to dimerize and activates the intracellular kinase domain presenting on each receptor, resulting in phosphorylation of tyrosine residues on each member of the receptor pair. Signalling complexes then form in the cytoplasm and activate gene transcription, which in turn induces responses such as cell proliferation [2]. The signalling pathway involves activation of *ras*, *raf* and mitogen-activated protein kinase (MAPK), which determine the activation of several nuclear proteins that regulate cell cycle progression from G1 to S phase. Evidence for the elevated production and expression of both EGFR and its activating ligands by the tumor cells, as a mechanism of EGFR activation is found in many tumors including cancers of the head and neck, oesophagus, stomach, pancreas, ovary, cervix, breast, lung, kidney and bladder (Table 1) [3-5]. In addition, EGFR is involved in the pathogenesis of many tumors and is a proven target for cancer therapy [6]. Therefore, removal of receptor stimulation can halt cell cycle progression and induce apoptosis, so EGFR is the key factor of the cancer therapy.

Cetuximab (C225, anti-EGFR mAb) is a 152 kDa molecule composed of four polypeptide chains: two identical heavy chains, each consisting of 449 amino

acids and two identical light chains, each consisting of 214 amino acids, which is a chimeric monoclonal antibody that specifically binds to the EGFR with a high affinity. Although Cetuximab also induces dimerization, unlike the TGF- $\alpha$  or EGF, this process does not result in activation of the tyrosine kinase leading to phosphorylation. Once bound, the 'inactivated' receptor-mAb complex is rapidly internalized, preventing further exposure of the receptor. For that reason, Cetuximab also inhibits growth factor-induced activation of downstream MAPK. As a result, the cellular processes necessary for proliferation and metastasis do not ensue, tumor growth is inhibited, and in many EGF-receptor-dependent cancers, cells undergo apoptosis. There is a strong correlation between Cetuximab concentrations sufficient to block MAPK activation and those that inhibit cell proliferation, and thereby kills the cancer cells [7-9] (Fig. 1-b). The efficacy of Cetuximab has been investigated in several clinical trials with various solid tumor malignancies.

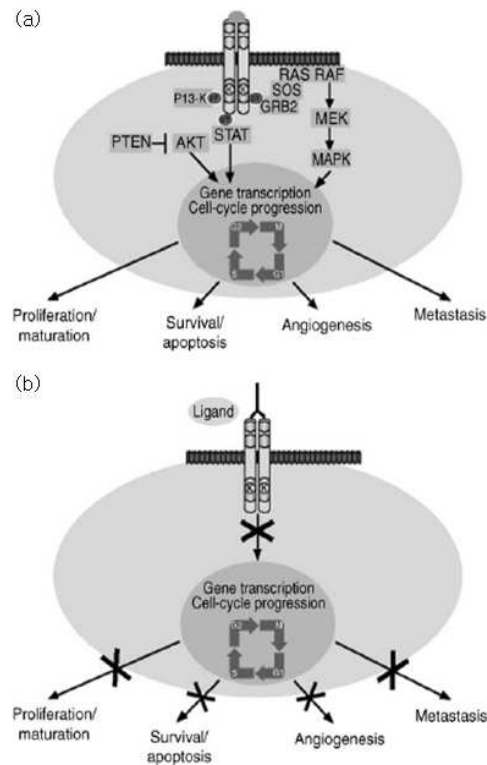


**Fig. 1. Cetuximab functions in the signal transduction mediated by epidermal growth factor receptor.**

(a) EGFR signal transduction pathway (activation of the MAPK cascade by EGFR) is initiated when a growth factor induces receptor dimerization and phosphorylation. Grb2 complex and the associated guanine nucleotide exchange factor Sos activate the small G protein Ras. The EGFR signalling network then stimulates multiple cellular responses including proliferation, survival, angiogenesis and metastasis. (b) Cetuximab binds to the EGFR, blocking growth factors from both accessing the receptor and stimulating EGFR signal transduction pathways. MAPK, mitogen activated protein kinase; EGFR, epidermal growth factor receptor.

**Table 1 EGFR over-expressing rate of cancers**

Tumor	EGFR over-expression (%)
Squamous cell head and neck cancer	80-100
Colorectal cancer	70-90
Nonsmall cell lung cancer	40-80
Gastric cancer	20-80
Pancreatic cancer	30-90
Breast cancer	15-90
Ovarian cancer	35-70
Renal cancer	50-90
Glyomas	40-50
Prostatic cancer	40-80
Cervical cancer	80-100

Rivera F, Vega-villegas M E, Lopez-Brea M F. Cetuximab, its clinical use and future perspectives. *Anti-Cancer Drugs* 2008;19:99-113

Immuno-PET (Positron Emission Tomography), the combination of PET with monoclonal antibody (mAb), is an attractive novel option to improve diagnostic tumor characterization, because it combines the high sensitivity and resolution of a PET camera with the specificity of a mAb. In fact, each mAb targeting a specific tumor cell surface marker or extracellular matrix component is a candidate for use in immuno-PET. Immuno-PET is based on annihilation coincidence detection after labeling of a mAb or mAb fragments with a positron-emitting radionuclide. The emitted positron will travel a distance of a few millimeters, depending on the initial positron energy and the density of the surroundings. After having lost its kinetic energy, combining with an electron leads to the so-called annihilation process, yielding two photons each with an energy of 0.511 MeV emitted simultaneously in opposite directions. After administration of PET conjugates to a patient, the distribution of the compound was monitored by detection of annihilation photon pairs with a PET camera [10-12]. In addition, immuno-PET enables the confirmation of tumor targeting and the quantification of mAb accumulation. Therefore, well targeted immuno-PET imaging with mAb or mAb fragments has a greater role in the monitoring of radioimmunotherapy for dosage and response to treatment of cancer.

PET is a highly sensitive and quantitative nuclear imaging modality that has been used widely to clinically image. Fluorodeoxyglucose (FDG) has been most often imaged with PET. The molecule is the fluorine-18 ( $^{18}\text{F}$ ,  $T_{1/2} = 109.8$  min) radiolabelled glucose analogue tracer, which was developed to image glucose metabolism. Cancer cells are known to have higher rates of glucose uptake than normal cells. The measurement of glucose metabolism as

a surrogate marker of tumor activity and cell number has been utilized for a number of applications in cancer management, including cancer staging, response assessment, prognostic evaluation and radiotherapy treatment planning [13].

Copper-64 ( $^{64}\text{Cu}$ ), as a positron emitter, is suitable for the targeting and clearance kinetics of the mAb due to its half life ( $T_{1/2} = 12.7$  hr) and the biological behavior of  $^{64}\text{Cu}$  complexes in PET imaging [14,15].  $^{64}\text{Cu}$ -labeled molecules has a high stability *in vitro*, because macrocyclic chelators are generally used as bifunctional chelators (DOTA, TETA, etc.) to bind Copper to antibodies and peptides [16,17]. The negatively charged complex showed that low liver uptake and rapid clearance through the kidneys. In addition, the neutral compound behaved similarly to the negatively charged, whereas the positively charged complexes showed higher retention in the kidney and liver out to 24 hr postinjection [18].

The importance of Gallium-68 ( $^{68}\text{Ga}$ ) from Germanium-68 ( $^{68}\text{Ge}$ )/ $^{68}\text{Ga}$  generator for PET imaging has recently increased [19]. The short half life and hydrophilic character of  $^{68}\text{Ga}$  ( $T_{1/2} = 67.6$  min) are appropriate for PET imaging. In addition,  $^{68}\text{Ga}$  has a strong point for PET over other cyclotron-produced positron emitters because it can be easily obtained by use of a commercially available  $^{68}\text{Ge}/^{68}\text{Ga}$  generator. The  $^{68}\text{Ge}$  has a long half life (270.8 d), allowing its use as a generator for more than one year [20-25]. Radionuclide generator systems are an important equipment in nuclear medicine as convenient methods for in-house generation of radionuclides which have short half life [26].

According to the studies, 1,4,7,10-tetraazacyclododecane-tetraacetic acid

(DOTA), one of the bichelating agent, is suitable for the metal chelating complex including gallium [23,27,28]. In fact, the functionalized DOTA can be easily conjugated with peptides, not with proteins, because of the boiling procedure for DOTA conjugation. Therefore, DOTA is not acceptable chelating agent for conjugation with proteins such as antibody. In the recent study, however, 1,4,7-triazacyclononane-1,4,7-triacetic acid (NOTA), as a bifunctional chelating agent, has been reported to form a highly stable neutral complex with gallium [29]. In addition, many researchers have reported that functionalized NOTA derivatives suitable for conjugation with proteins or peptides [30-33]. In some functionalized NOTA, S-2-(4-Isothiocyanatobenzyl)-1,4,7-Triazacyclononane-1,4,7-triacetic acid (scn-Bz-NOTA) is a bifunctional chelating agent which is particularly useful for PET imaging with  $^{68}\text{Ga}$ . The reactive isothiocyanato group of NOTA reacts readily with surface amino groups of proteins or nucleophilic groups of other polymers.

Herein, to produce an imaging agent targeted to the EGFR over-expressing cancer for immuno-PET, the immunoreactivity of antibody fragments of anti EGFR antibody was examined, and, at the same time, the cell lines over-expressing EGFR was confirmed. The Cetuximab Fab fragments were radiolabeled with  $^{68}\text{Ga}$  using a NOTA bifunctional chelator. Moreover, biodistribution of  $^{68}\text{Ga}$ -NOTA-Cetuximab Fab fragments was analysed and PET images were acquired in EGFR over-expressing cancer xenografts.

## **II. MATERIALS AND METHODS**

### **1. Cell line**

A549 human lung cancer cells were cultured in RPMI-1640 supplemented in 10% Fetal Bovine Serum (FBS) and antibiotics (100 U/ml penicillin G and 100  $\mu\text{g/ml}$  streptomycin). CT26 mouse colon cancer cells were cultured in DMEM with 10% FBS and antibiotics. These two cell lines were grown at 37°C in a 5% CO<sub>2</sub> and 95% air humidified atmosphere.

### **2. Evaluation of EGFR expression in cancer cells**

#### **2.1. Reverse transcriptase-polymerase chain reaction**

Total RNA was prepared from A549 and CT26 cells with the total RNA extraction kit (iNtRON Biotechnology, Inc., Korea) according to the provided protocol. The cDNA synthesis from the extracted total RNA was performed with SuperScript III First-strand synthesis system for a RT-PCR kit (Invitrogen, USA). Two microgram of total RNA (1  $\mu\text{l}$ ), 10  $\mu\text{M}$  oligo (dT) (1  $\mu\text{l}$ ), 10 mM dNTP mix (1  $\mu\text{l}$ ) and diethylpyrocarbonate (DEPC)-treated water (7  $\mu\text{l}$ ) were incubated at 65°C for 5 min, then placed on ice for 1 min. After incubation, 10X reverse transcriptase buffer (2  $\mu\text{l}$ ), 25 mM MgCl<sub>2</sub> (4  $\mu\text{l}$ ), 0.1 M dithiothreitol (DTT) (2  $\mu\text{l}$ ), 40 U RNaseOUT (1  $\mu\text{l}$ ), 200 U Superscript III

RT (1  $\mu\text{l}$ ), and cDNA synthesis mix (10  $\mu\text{l}$ ) were incubated at 50°C for 50 min and next at 85°C for 5 min. The reaction was terminated by chilling on ice. One microliter of RNase H was added to the tube, which was then incubated at 37°C for 20 min. The synthesized cDNA was amplified using a thermal cycler with the following cycle parameters: denaturation at 94°C for 1 min; annealing at 50°C for 30 sec; and extension at 72°C for 90 sec. After 35 cycles of amplification, the PCR products were extended at 72°C for 7 min. The cDNA amplification was monitored by gel electrophoresis in a 2% ethidium bromide-stained agarose gel.

## **2.2. Western blotting**

A549 and CT26 cells ( $5 \times 10^6$  cells) were lysed in a cell lysis buffer (M-PER Mammalian Protein Extraction Reagent, Pierce, USA) with protease inhibitor cocktail for 1 hr in 4°C cold chamber. The cellular whole cell protein concentrations were determined by the micro-protein assay (DC Protein Assay, Bio-Rad, USA), measuring at 655 nm of wavelength with microplate reader 550 (Bio-Rad, USA). The extracted proteins (100  $\mu\text{g}$ ) were separated on a 4 ~ 15% SDS-polyacrylamide gel (100 V, 70 min) and transferred (100 V, 1 hr, 4°C) to nitrocellulose membranes (Micron separations Inc., USA). The membranes were blocked with a casein blocker (Bio-Rad, USA) on a rocker for overnight in 4°C cold chamber and triple-washed with TBST (Tris-buffered saline tween 20) for 10 min. The washed membrane was incubated with a 1:200 dilution of the anti-EGFR rabbit polyclonal antibody (sc-03, Santa Cruz Biotechnology, USA) for 2 hr at room temperature and triple washed with

TBST for 10 min. The membranes were incubated with a 1:1,000 dilution of the horseradish peroxidase conjugated to anti-rabbit IgG for 1 hr at room temperature and triple washed with TBST for 10 min. Finally, the blots on the membranes were developed by enhanced chemiluminescence (ECL Western Blotting Detection Reagents, Amersham, UK). The anti-glyceraldehyde 3-phosphate dehydrogenase (GAPDH) rabbit polyclonal antibody was used as a loading control.

### **2.3. Immuno-cytochemistry**

A549 and CT26 cells ( $1 \times 10^5$  cells) were incubated for overnight on 24-well plates with coverslips, and the washed with cold PBS. The cells were incubated with 5  $\mu$ g of Cetuximab at room temperature for 1 hr. After incubation, the washed cells with cold PBS were incubated in dark at room temperature for 1 hr with FITC labeled anti-human IgG (polyclonal rabbit anti-human IgG/FITC Rabbit F(ab')<sub>2</sub>, DakoCytomation, Denmark). After triple-washing with cold PBS the cells on each coverslip were observed with a fluorescence microscope (IX71, Olympus, Japan)

**Table 2 Primer sequence information**

Primer	Sequence
Human $\beta$ -actin (f)	GTG GGG CGC CCC AGG CAC CAG GGC
Human $\beta$ -actin (r)	CTC CTT AAT GTC ACG CAC GAT TTC
Mouse $\beta$ -actin (f)	AGG CTG TGC TGT CCC TGT ATG C
Mouse $\beta$ -actin (r)	ACC CAA GAA GGA AGG CTG GAA A
EGFR (f)	GAG AGG AGA ACT GCC AGA A
EGFR (r)	GTA GCA TTT ATG GAG AGT G

### **3. Tumor model**

The 5-week-old female athymic nude mice (BALB/cSlc-nu, Japan SLC, Inc., Japan) were housed as 5 heads/cage. The mice were given food and water ad libitum and were kept on a 12 hr light/12 hr dark photoperiod cycle regime. Mice were allowed to acclimate for a week prior to the study. The animals were handled in accordance with the guidelines of the Korea Institute of Radiological and Medical Sciences.

A549 cells were harvested by incubation with 0.5% trypsin-EDTA for 5 min. The cells were pelleted by centrifugation at 1,000 rpm for 3 min and resuspended in serum-free media. The cells ( $1 \times 10^7$  cells/head; single-cell suspensions of over 98% viability as determined by trypan blue exclusion) were subcutaneously implanted into the right back thigh of the 6-week-old athymic nude mice. The mice were raised for 4~5 weeks until tumors reached roughly 1 cm in diameter to study biodistribution and immuno-PET imaging of the radiolabeled antibody fragments.

#### 4. Preparation of Cetuximab Fab fragments

Cetuximab was purchased from Merck Inc. (Germany), and the Fab of Cetuximab was prepared by the papain digestion method using Immunopure Fab preparation kit (Pierce, USA). Cetuximab was concentrated with a vivaspin 20 (50,000 MWCO, Sartorius, Germany) in a digestion buffer at pH 7.0 (42 mg of cysteine · HCl in 12 ml of phosphate buffer at pH 10). The immobilized papain (Pierce, USA) was twice washed with 4 ml of the digestion buffer and resuspended in 0.5 ml of the digestion buffer in a test tube. The prepared 10 mg/ml of Cetuximab was added in the test tube and incubated for 12 hr at 37°C in a shaker water bath. The crude digest was separated from the immobilized papain using a separator tube, and then loaded on an Immobilized protein A column (Pierce, USA). The protein concentrations of eluted fractions were detected by the micro-protein assay (DC Protein Assay, Bio-Rad, USA), measuring at 655 nm of wavelength with the microplate reader 550 (Bio-Rad, USA). The purity of Cetuximab Fab fragments were assessed by sodium dodecyl sulfate-polyacrylamide gel electrophoresis (SDS-PAGE). Cetuximab (5 µg) and Cetuximab Fab fragment (5 µg) sample were diluted with Laemmli sample buffer contained of β-mercaptoethanol and boiled for 5min, and then the samples were loaded in 12% acrylamide gel. 80V; 20min, 100V; 1hr (EPS 2A200, Amersham, USA). The PageRuler™ Plus Prestained Protein Ladder (Fermentas, Canada) was used as a protein molecular weight marker. The Cetuximab Fab fragments were dialyzed using a dialysis membrane 3,500 MWCO (Spectrapore, USA) against a 50 mM sodium phosphate buffer (pH 7.5) for overnight at 4°C and then stored at -20°C.

## **5. Preparation of the radiolabeled Cetuximab and Cetuximab Fab fragments**

### **5.1. Radiolabeling of Cetuximab and Cetuximab Fab fragments with iodine-125**

Iodination of the Cetuximab and Cetuximab Fab fragments was accomplished using the Iodo-beads method. Two Iodo-beads were washed with 1 ml of 0.1 M sodium phosphate buffer (pH 7.5) and dried on filter paper. Each beads was placed in 1.5 ml tube with a magnetic stirring bar. The 100  $\mu$ Ci of iodine-125 ( $\text{Na}^{125}\text{I}$ ; purchased from Perkin Elmer, USA) and 50 mM sodium phosphate buffer (pH 7.5) were added in each tube up to 300  $\mu$ l, and then pre-incubated at room temperature for 30 min. After pre-incubation, 100  $\mu$ g of Cetuximab or Cetuximab Fab fragments in 100  $\mu$ l of 50 mM sodium phosphate buffer (pH 7.5) was added to the  $^{125}\text{I}$  solution, which was then incubated at room temperature for 30 min. The reaction was terminated by removing the Iodo-bead. The labeling yield was determined by instant thin layer chromatography (ITLC) using a silica gel (SG) coated sheet and acetone as a developing solution.

## 5.2. NOTA conjugation to Cetuximab Fab fragments

The Cetuximab Fab fragments, as a substrate for conjugation with S-2-(4-Isothiocyanatobenzyl)-1,4,7-triazacyclononane-1,4,7,-triacetic acid (SCN-Bz-NOTA), were dialyzed in dialysis membrane 3,500 MWCO (Spectrapore, USA) against a 0.1 M sodium borate buffer (pH 8.5). Dialyzed Cetuximab Fab fragments were concentrated with a vivaspin 20 (10,000 MWCO, Sartorius, Germany) and was quantified by the micro-protein assay as described earlier. Five milligram of Cetuximab Fab fragments (below 1 ml) was added to 1.5 ml tube with a magnetic stirring bar. The SCN-Bz-NOTA was dissolved in dimethylsulfoxide (DMSO) at a concentration of 5 mM, which was then added to the Cetuximab Fab fragments with 10 fold molar excess. The resulting reaction mixtures were incubated at 4°C for 24 hr (DMSO concentration below 2% in the reaction mixture). After conjugation, the reaction mixture was dialyzed with the dialysis membrane 3,500 MWCO (Spectrapore, USA) against a 10 mM sodium acetate buffer (pH 6.5) at 4°C for overnight in order to remove the free SCN-Bz-NOTA. The Fab-NOTA was quantified by the micro-protein assay and then stored at -20°C.

## 5.3. Radiolabeling of NOTA-Cetuximab Fab fragments with Gallium-68

$^{68}\text{Ga}$  was available from a  $^{68}\text{Ge}/^{68}\text{Ga}$  generator system (Cyclotron Co., Ltd, Obninsk, Russia), where  $^{68}\text{Ge}$  was attached. The  $^{68}\text{Ga}$  was eluted with 6 ml of 0.1 M HCl and then 5 ml of 30% HCl was added to the generator eluate (the

final HCl concentration was 4.0 M). The mixed  $^{68}\text{Ga}$  solution of 11 ml was passed through an anion exchange column (SPE cartridge Chromafix 30-PS-HCO<sub>3</sub>, Machanery-Nagel, Germany) at a flow rate of 4 ml/min at room temperature, which trapped  $^{68}\text{Ga}$  in the anion exchange column. The  $^{68}\text{Ga}$  was then eluted with 10 fractions of deionized water (10×50  $\mu\text{l}$ ) at a flow rate of 0.5 ml/min. The radio-activities of fractions were checked by the Radioisotope calibrator (CRC-127R, CAPINTEC, USA). The purified  $^{68}\text{Ga}$  (0.5 ~ 1 mCi below 50  $\mu\text{l}$ ) was adjusted against pH 4.2 using 1 N NaOH. One hundred microgram of NOTA-conjugated Cetuximab Fab fragments in 100 mM sodium acetate buffer (pH 6.5) was added to the  $^{68}\text{Ga}$  solution and then incubated at room temperature for 30 min. The labeling yield was determined by instant thin layer chromatography (ITLC) using a silica gel (SG) coated sheet and 20 mM citric acid (pH 5.0) 50 mM EDTA as a developing solution.

#### **5.4. *In vitro* stability test of $^{68}\text{Ga}$ -NOTA Cetuximab Fab fragments**

*In vitro* stability of  $^{68}\text{Ga}$ -NOTA-Cetuximab Fab fragments were analysed in the presence of an equivalent of human serum. The mixtures of serum and  $^{68}\text{Ga}$ -NOTA-Cetuximab Fab fragments were incubated at 37°C. At varied time points (0, 10, 20, 30, 45, 60 min), radiolabeling stability of the conjugates was determined by ITLC using a silica gel coated sheet and 20 mM citric acid (pH 5.0) containing 50mM EDTA as a developing solution.

## 6. *In vitro* cellular binding test

A549 and CT26 cells ( $1 \times 10^6$ ) were washed 3 times with cold PBS. The cells for non-specific binding were pre-incubated with 10  $\mu\text{g}$  of cold Cetuximab at room temperature for 1 hr. The cells were incubated for 1 hr at room temperature with  $^{125}\text{I}$ -Cetuximab,  $^{125}\text{I}$ -Cetuximab Fab fragments or  $^{68}\text{Ga}$ -NOTA-Cetuximab Fab fragments (0.66 pmole/100  $\mu\text{l}$  PBS). The treated cells were washed with cold PBS, and the remaining radioactivity of the washed cells were measured with a Wallac Wizard 3" 1480 automatic gamma counter (Perkin Elmer, USA).

## **7. Biodistribution assay of <sup>68</sup>Ga-NOTA-Cetuximab Fab fragments and <sup>125</sup>I-Cetuximab Fab fragments in EGFR over-expressing cancer xenograft mice**

Mice bearing subcutaneous EGFR over-expressing cancer xenograft were prepared different sets of biodistribution experiments. In the first experiment, 15 mice were injected with <sup>125</sup>I-Cetuximab Fab fragments (20  $\mu$ g, 100  $\mu$ l, 740 KBq) through the tail vein. At 10 min (n=3), 30 min (n=4), 1 hr (n=4) and 2 hr (n=4) after injection, the mice were anesthetized, and then major organs were removed. In the second experiment, 16 mice were injected with <sup>68</sup>Ga-NOTA-Cetuximab Fab fragments (20  $\mu$ g, 100  $\mu$ l, 1.1 MBq) through the tail vein. At 30 min (n=4), 1 hr (n=4), 2hr (n=4) and 3 hr (n=4) after injection, the mice were anesthetized, bled killed, and dissected, and then the major organs were collected. Their radioactivities were counted in a Wallac Wizard 3" 1480 automatic gamma counter (Perkin Elmer, USA). The radioactivity of each organ was represented as percentage injected dose per gram (%ID/g) of organ.

## **8. Small animal PET imaging of $^{68}\text{Ga}$ -NOTA-Cetuximab Fab fragments in EGFR over-expressing cancer xenograft mice**

Mice bearing subcutaneous EGFR over-expressing cancer xenografts were injected with  $^{68}\text{Ga}$ -NOTA-Fab (100  $\mu\text{g}$ , 200  $\mu\text{l}$ , 5.6 MBq) through the tail vein. After 1 and 3 hr post injection, small animal PET images were obtained for 30 min using the micro PET R4 rodent model scanner (Concorde Microsystems Inc. USA). The injection was performed after the mice had been anesthetized with 2% isoflurane.

### **III. RESULTS**

#### **1. Evaluation of EGFR expression in cancer cells**

The RT-PCR analysis, Western blotting and immuno-chemistry study were performed to evaluate EGFR expression in A549 and CT26 cells. In the RT-PCR analysis, the cDNA synthesized from mRNA of A549 and CT26 cells was analysed by gel electrophoresis in a 2% ethidium bromide-stained agarose gel. The cDNA sequence of EGFR was effectively amplified from mRNA of A549 cells (454 bp), but not from that of CT26 cells (Fig. 2).

According to the Western blotting analysis of EGFR protein expression, the EGFR was highly expressed in the A549 cells, but little in the CT26 cells (Fig. 3). EGFR expression on the surface of the tumor cells was also examined by immunostaining with fluorescence-labelled Cetuximab. The labelled Cetuximab was able to effectively bind to the surface of A549 cells, not to that of CT26 cells (Fig. 4). According to these data, the EGFR over-expressing A549 cells were utilized as an *in vitro* and *in vivo* tumor model in this study. The CT26 cells were used as a negative control of tumor cells.

#### **2. Fragmentation of Cetuximab Fab fragments**

Cetuximab antibodies were treated with papain to make their Fab fragments. The Fab fragmentation of Cetuximab was assessed by SDS-PAGE. The undigested Cetuximab exhibited two bands of a heavy chain (50 Kd) and

a light chain (25 Kd) (Fig. 5). Meanwhile, the digested Cetuximab showed a thicker single band, presumably consisting of a light chain and a digested heavy chain. The digested Cetuximab Fab fragments were used for conjugation of chelators for radioisotope without further purification steps.

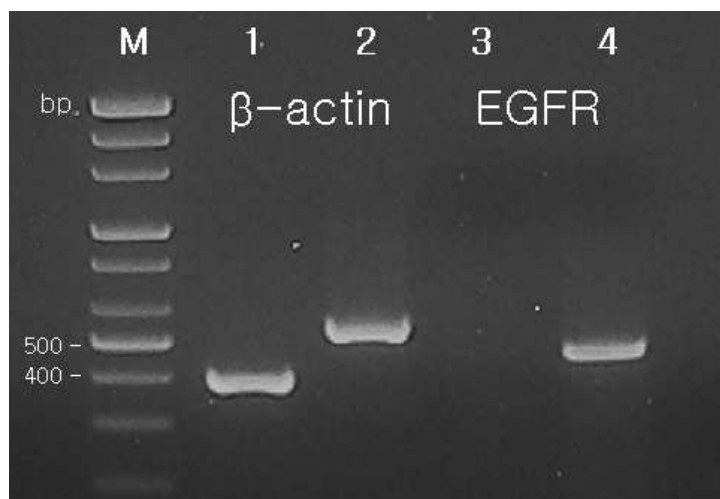


**Figure 2. Analysis of EGFR expression in A549 and CT26 cells by RT-PCR.** PCR products of EGFR cDNA synthesized from mRNA of A549 (lane 2,4) and CT26 cells (lane 1,3) were analyzed by agarose gel electrophoresis. M; 100 bp DNA Ladder (GenePia, Korea), Lane 1; mouse  $\beta$ -actin of CT26 (395 bp), lane 2; human  $\beta$ -actin of A549 (546 bp), lane 3; EGFR of CT26, lane 4; EGFR of A549 (454 bp).

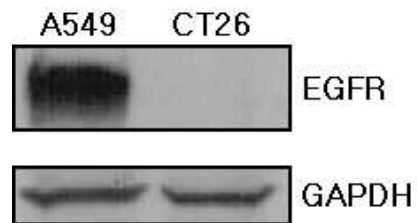


**Figure 3. Analysis of EGFR expression in A549 and CT26 cells by Western blotting.**

The presence of EGFR in the lysates of A549 and CT26 cells was analyzed by Western blotting with Cetuximab. The glyceraldehyde 3-phosphate dehydrogenase (GAPDH) was used as a loading control.

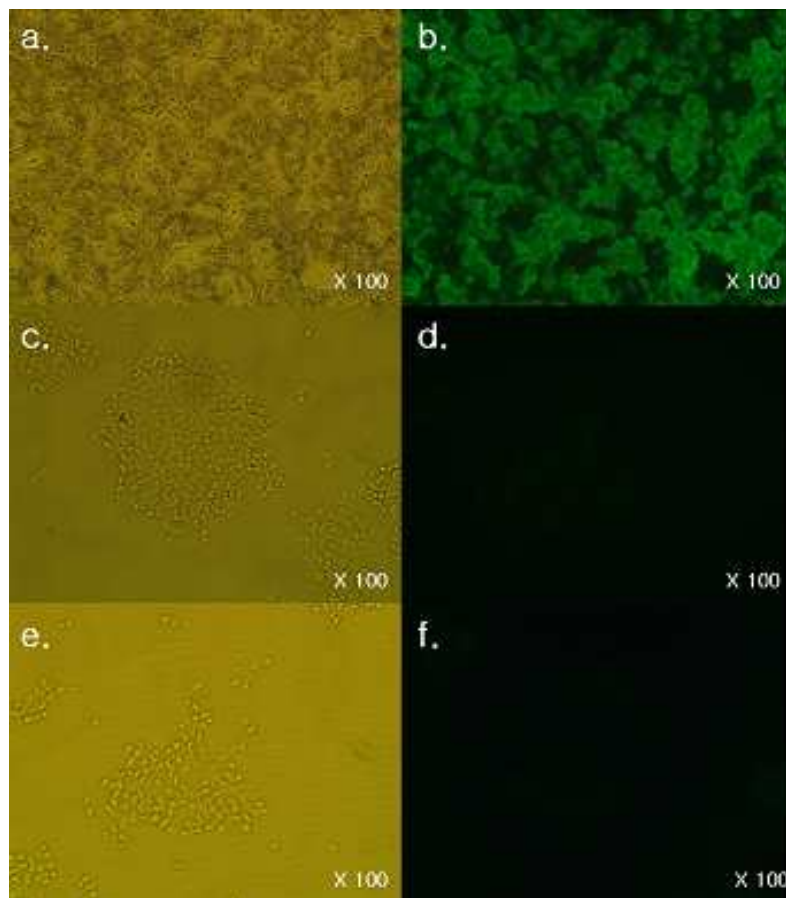


**Figure 4. Analysis of EGFR expression in A549 and CT26 cells by immunocytochemical staining with Cetuximab.**

A549 (a-d) and CT26 cells (e,f) were stained with fluorescence-labelled Cetuximab. The tumor cells treated (a,b,e,f) or untreated (c,d) with Cetuximab were examined with a light microscopy (a,c,e) and a fluorescence microscopy (b,d,f).

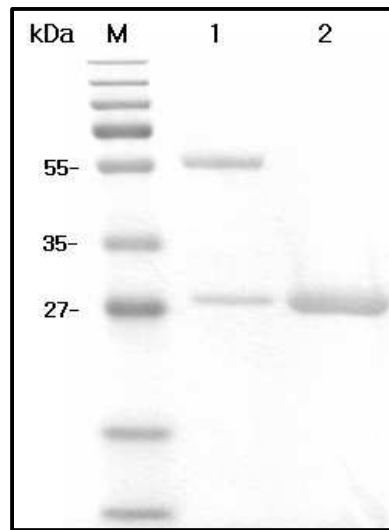


**Fig. 5. Analysis of Cetuximab Fab fragments by SDS-PAGE.**

Undigested Cetuximab (lane 1) and papain-digested Cetuximab (lane 2) were analyzed by SDS-PAGE. M; prestained protein molecular weight marker.

### **3. Radiolabeling of Cetuximab and Cetuximab Fab fragments with I-125 and Ga-68**

Cetuximab and Cetuximab Fab fragments were labeled with iodine-125 for indirect evaluation of immunoreactivity of papain-digested Cetuximab Fab fragments. Radiolabeling yields of the two proteins were over 95% (data not shown).

The conjugate of NOTA-Cetuximab Fab fragments was also labeled with Gallium-68 for *in vivo* biodistribution analysis and immunPET imaging. The yield of <sup>68</sup>Ga-labeling to the Fab fragments was estimated to be also over 95% (Fig. 6). Since the radiolabeled products had a high chemical purity, they were used for *in vitro* and *in vivo* tests without further purification.

### **4. *In vitro* characterization of <sup>68</sup>Ga-NOTA-Cetuximab Fab fragments**

#### **4.1. Chemical stability of <sup>68</sup>Ga-NOTA-Cetuximab Fab fragments**

*In vitro* chemical stability of <sup>68</sup>Ga-NOTA-Cetuximab Fab fragments was examined in the presence of human serum at 37°C for 60 min. During the incubation, intactness of <sup>68</sup>Ga-NOTA-Cetuximab Fab fragments was assayed by ITLC-SG. Their radiochemical purity was  $97.73 \pm 1.31$ ,  $97.65 \pm 1.20$ ,  $97.67 \pm 0.97$ ,  $98.57 \pm 1.38$ ,  $97.64 \pm 2.29$  and  $92.76 \pm 2.28\%$  at 0, 10, 20, 30, 45 and 60 min of incubation, respectively (Fig. 7).

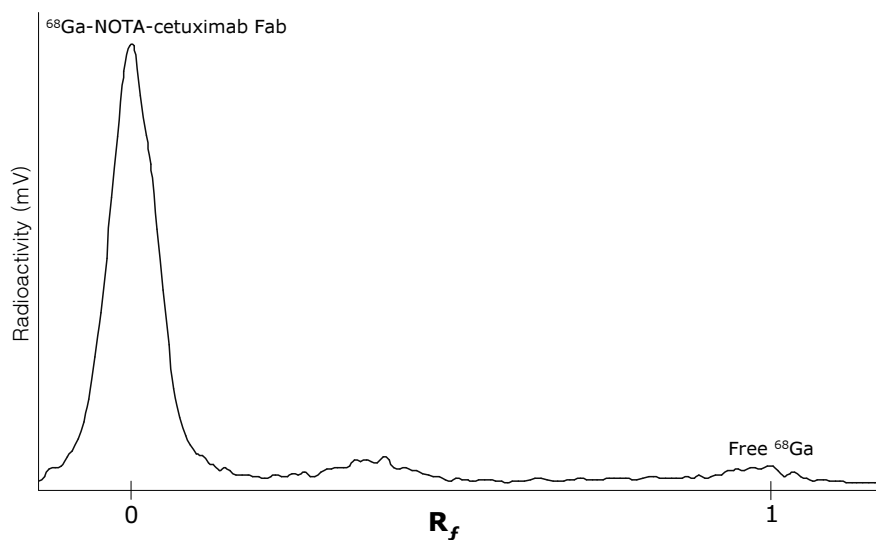


**Figure 6. Analysis of radiolabeling yield of <sup>68</sup>Ga-NOTA-Cetuximab Fab fragments by instant thin layer chromatography.**

After incubating NOTA-Cetuximab Fab fragments in a <sup>68</sup>Ga solution, the reaction mixture was run on a silica gel-coated sheet. <sup>68</sup>Ga-NOTA-Cetuximab Fab fragments remained on the starting point of the ITLC-SG sheet ( $R_f = 0$ ), but free <sup>68</sup>Ga moved to the end of the sheet ( $R_f = 1$ ). The radiolabeling yield of <sup>68</sup>Ga-NOTA-Cetuximab Fab fragments was estimated to be higher than 95%.

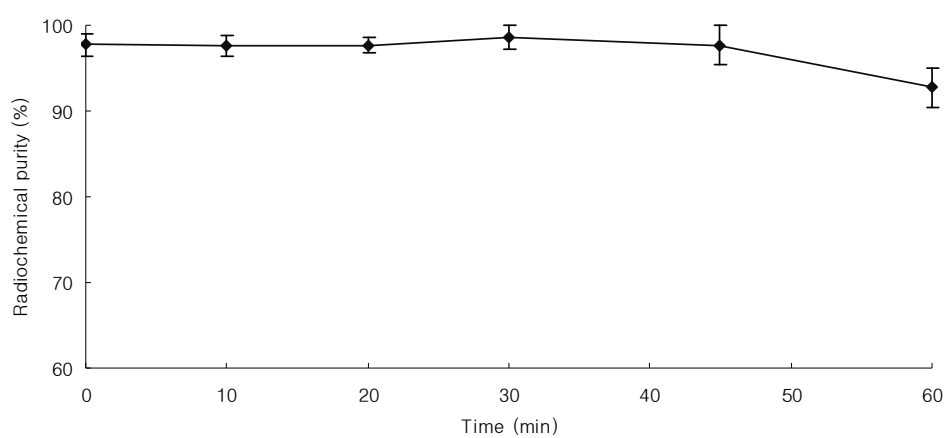


**Figure 7. In vitro chemical stability of  $^{68}\text{Ga}$ -NOTA-Cetuximab Fab fragments.**

The radiochemical purity of  $^{68}\text{Ga}$ -NOTA-Cetuximab Fab fragments was measured by ITLC-SG at 0, 10, 20, 30, 45 and 60 min of incubation with human serum.

## 4.2. Immunoreactivity of $^{68}\text{Ga}$ -NOTA-Cetuximab Fab fragments

A549 and CT26 cells were treated with  $^{68}\text{Ga}$ -NOTA-Cetuximab Fab fragments,  $^{125}\text{I}$ -Cetuximab, or  $^{125}\text{I}$ -Cetuximab Fab fragments to compare their immunoreactivities to each other. Generally, the Cetuximab derivatives have a higher binding affinity to A549 cells, but not to CT26 cells. Their binding amounts to A549 cells were 7.8%, 4.3%, and 4.3% of added dose of  $^{125}\text{I}$ -Cetuximab,  $^{125}\text{I}$ -Cetuximab Fab fragments, and  $^{68}\text{Ga}$ -NOTA-Cetuximab Fab fragments, respectively (Fig. 8). Meanwhile, their binding to CT26 was marginal, less than 1%.

Among the Cetuximab derivatives, the whole Cetuximab antibody exhibited approximately 2-fold higher immunoreactivity to the EGFR-overexpressing cells than its Fab fragments.  $^{125}\text{I}$ -Cetuximab Fab fragments and  $^{68}\text{Ga}$ -NOTA-Cetuximab Fab fragments exhibited the same amount of immunoreactivity. The relative immunoreactivities of  $^{125}\text{I}$ -Cetuximab Fab fragments and  $^{68}\text{Ga}$ -NOTA-Cetuximab Fab fragments were respectively 55.1% and 55.2% of  $^{125}\text{I}$ -Cetuximab. According to these data, conjugation of  $^{68}\text{Ga}$ -NOTA to the Cetuximab Fab fragments hardly affected its immunoreactivity.

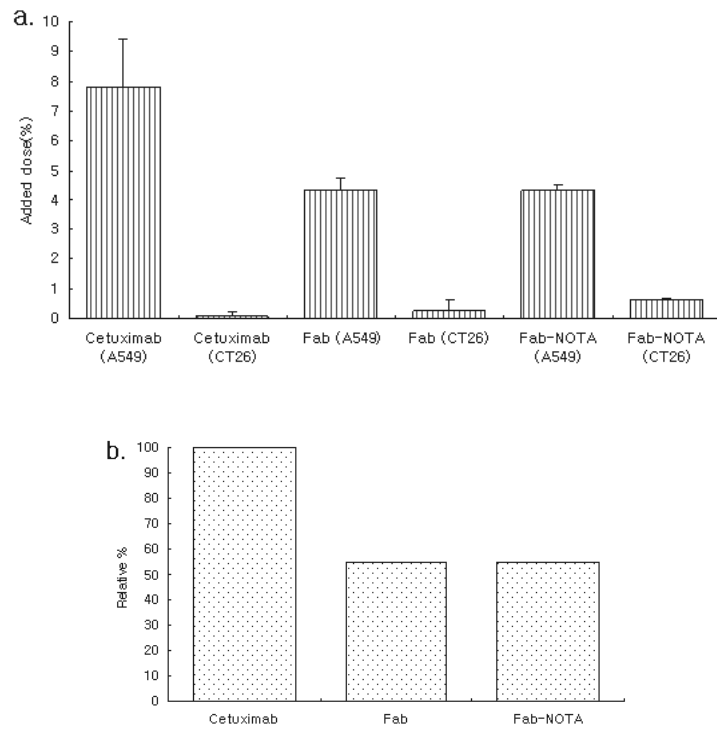


**Figure. 8. Cellular binding affinities of the radiolabeled Cetuximab derivatives**  
 $^{68}\text{Ga}$ -NOTA-Cetuximab Fab fragments,  $^{125}\text{I}$ -Cetuximab, or  $^{125}\text{I}$ -Cetuximab Fab fragments were added to A549 or CT26 cells. The radioactivities bound to the cells were counted (a) and compared to each other with A549 cells (b).

## **5. Biodistribution of radiolabeled Cetuximab Fab fragments**

### **5.1. Biodistribution of <sup>125</sup>I-Cetuximab Fab fragments**

<sup>125</sup>I-Cetuximab Fab fragments were intravenously administered to nude mice bearing A549 tumors overexpressing EGFR. At varied time points after injection, radioactivities of major organs (Blood, liver, lung, spleen, kidney, stomach, small intestine, large intestine, heart, thyroid, muscle, femur and tumor (A549)) were counted. The tumor (A549) uptake of <sup>125</sup>I-Cetuximab Fab fragments was  $3.30 \pm 0.10$ ,  $2.57 \pm 0.31$ ,  $2.66 \pm 0.22$ , and  $1.45 \pm 0.39$  %ID/g at 10, 30, 60, and 120 min postinjection, respectively (Table 3, Fig 9). <sup>125</sup>I-Cetuximab Fab fragments were highly accumulated in kidneys and stomach, but less in the other organs including tumor tissues. This data indicate rapid clearance of Cetuximab Fab fragments from the blood circulation.

### **5.2. Biodistribution of <sup>68</sup>Ga-NOTA-Cetuximab Fab fragments**

<sup>68</sup>Ga-NOTA-Cetuximab Fab fragments were intravenously administered to nude mice bearing A549 tumors overexpressing EGFR. At varied time points after injection, radioactivities of major organs were counted. The tumor uptake of <sup>68</sup>Ga-NOTA-Cetuximab Fab fragments was  $3.19 \pm 0.40$ ,  $4.28 \pm 0.57$ ,  $5.78 \pm 0.46$  and  $5.31 \pm 0.14$  %ID/g at 30, 60, 120 and 180 min post injection (Table 4, Fig 10). <sup>68</sup>Ga-NOTA-Cetuximab Fab fragments were heavily cleared away through kidneys ( $35.14 \pm 2.31$ ,  $44.19 \pm 2.40$ ,  $59.38 \pm 4.22$  and  $59.53 \pm 8.93$  %ID/g at 30, 60, 120 and 180 min, respectively). This data implied that the

renal route is a predominant clearance system for the  $^{68}\text{Ga}$ -labeled Fab fragments.

**Table 3. Biodistribution of <sup>125</sup>I-Cetuximab Fab fragments in mice**

Organ	Unit : %ID/g			
	10 min	30 min	60 min	120 min
Blood	10.81 ± 0.15*	6.52 ± 1.08	5.36 ± 0.19	2.88 ± 0.76
Liver	4.34 ± 0.24	2.86 ± 0.46	2.22 ± 0.22	1.25 ± 0.21
Lung	6.96 ± 0.05	4.54 ± 1.04	3.91 ± 0.18	2.19 ± 0.66
Spleen	3.75 ± 0.25	2.39 ± 0.38	2.21 ± 0.21	1.12 ± 0.40
Kidney	18.73 ± 3.42	20.03 ± 4.12	12.40 ± 1.56	5.19 ± 1.95
Stomach	16.79 ± 4.46	26.46 ± 11.34	27.76 ± 6.79	19.64 ± 4.61
S. Intestine	2.84 ± 0.13	2.90 ± 0.71	2.89 ± 0.30	2.46 ± 0.62
L. Intestine	1.99 ± 0.15	1.72 ± 0.20	1.77 ± 0.16	2.05 ± 0.34
Heart	3.34 ± 0.42	2.25 ± 0.45	2.16 ± 0.30	1.20 ± 0.36
Thyroid	0.79 ± 0.22	1.48 ± 0.34	2.51 ± 1.15	2.87 ± 0.74
Muscle	2.20 ± 0.09	1.72 ± 0.34	1.52 ± 0.15	1.12 ± 0.25
Femur	2.74 ± 0.37	2.12 ± 0.35	2.00 ± 0.13	1.11 ± 0.13
Tumor(A549)	3.30 ± 0.10	2.57 ± 0.31	2.66 ± 0.22	1.45 ± 0.39

\*Data represent mean ± SD (n=three or four animals).

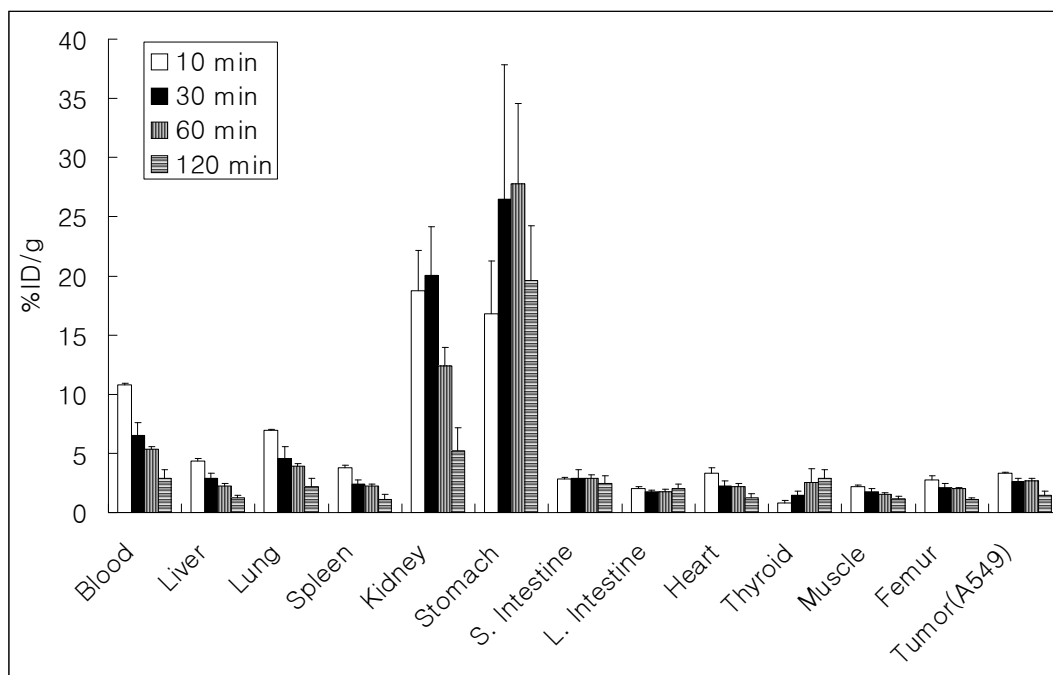


**Figure 9. Biodistribution of <sup>125</sup>I-Cetuximab Fab fragments in mice.**

<sup>125</sup>I-Cetuximab Fab fragments were intravenously administered to nude mice bearing A549 tumors. At 10, 30, 60, and 120 min after injection via tail vein, radioactivities of major organs were counted. Each values present mean %ID/g, and error bars present SD.

**Table 4. Biodistribution of <sup>68</sup>Ga-NOTA-Cetuximab Fab fragments in mice**

Organ	Unit : %ID/g			
	30 min	60 min	120 min	180 min
Blood	24.40 ± 7.62*	12.54 ± 0.79	11.13 ± 1.22	10.09 ± 0.62
Liver	31.02 ± 8.00	27.91 ± 3.11	40.05 ± 6.35	41.50 ± 3.68
Lung	15.18 ± 4.17	9.76 ± 1.57	10.47 ± 2.87	8.52 ± 0.94
Spleen	22.56 ± 9.16	22.40 ± 4.49	21.13 ± 2.73	16.50 ± 1.76
Kidney	35.14 ± 2.31	44.19 ± 2.40	59.38 ± 4.22	59.53 ± 8.93
Stomach	0.96 ± 0.59	0.66 ± 0.21	1.15 ± 0.45	1.02 ± 0.87
S. Intestine	3.79 ± 1.57	2.90 ± 0.06	5.09 ± 2.77	6.00 ± 1.69
L. Intestine	1.83 ± 1.29	1.10 ± 0.15	3.78 ± 1.69	5.90 ± 2.21
Heart	9.01 ± 3.37	5.62 ± 0.79	5.11 ± 0.86	4.95 ± 0.19
Thyroid	0.28 ± 0.14	0.20 ± 0.10	0.26 ± 0.06	0.20 ± 0.08
Muscle	2.35 ± 0.34	2.08 ± 0.44	2.43 ± 0.35	2.88 ± 0.62
Femur	6.44 ± 4.05	5.87 ± 0.45	6.37 ± 1.99	8.01 ± 3.19
Tumor(A549)	3.19 ± 0.40	4.28 ± 0.57	5.78 ± 0.46	5.31 ± 0.14

\*Data represent mean ± SD (n=four animals).

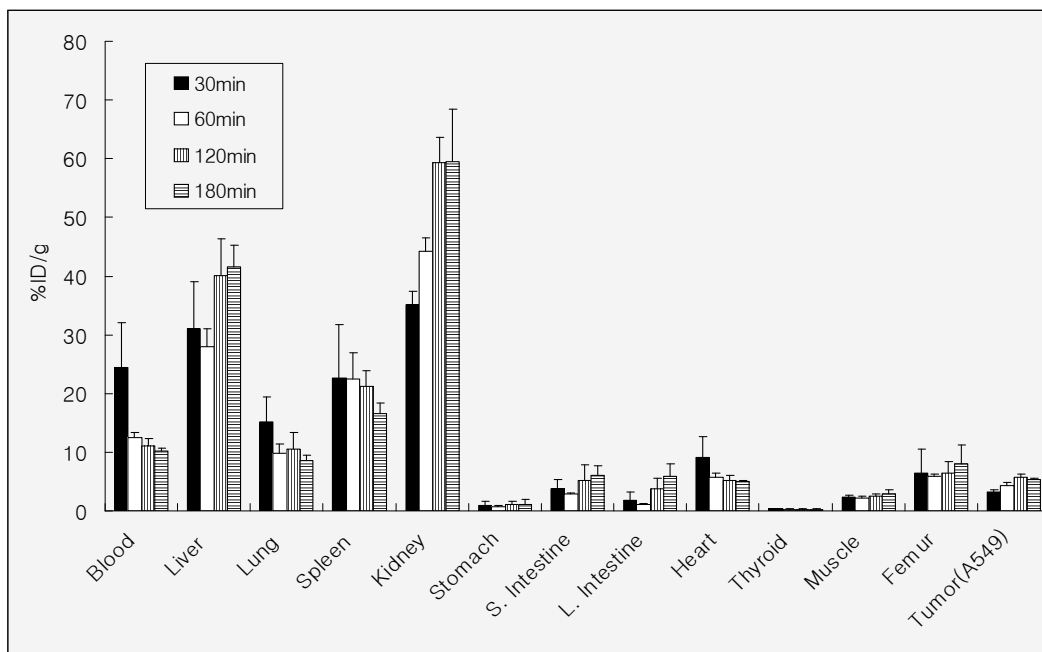


**Figure 10. Biodistribution of <sup>68</sup>Ga-NOTA-Cetuximab Fab fragments in mice.**

<sup>68</sup>Ga-NOTA-Cetuximab Fab fragments were intravenously administered to nude mice bearing A549 tumors. At 30, 60, 120, and 180 min after injection via tail vein, radioactivities of major organs were counted. Each values present mean %ID/g, and error bars present SD.

## **6. Immuno-PET imaging with $^{68}\text{Ga}$ -NOTA-Cetuximab Fab fragments in mice bearing EGFR over-expressing cancer xenograft**

Immuno-PET images of mice bearing A549 tumors were acquired at 1 hr (Fig. 11) and 3 hr (Fig. 12) post injection of  $^{68}\text{Ga}$ -Cetuximab Fab fragments. The transverse, coronal and sagittal PET images were obtained through normalization and correction of time and decay. The administered  $^{68}\text{Ga}$ -Cetuximab Fab fragments were heavily localized in the liver, kidneys, and bladder. At the same time, rather specific localization in tumor tissues was also seen in the both immuno-PET images.

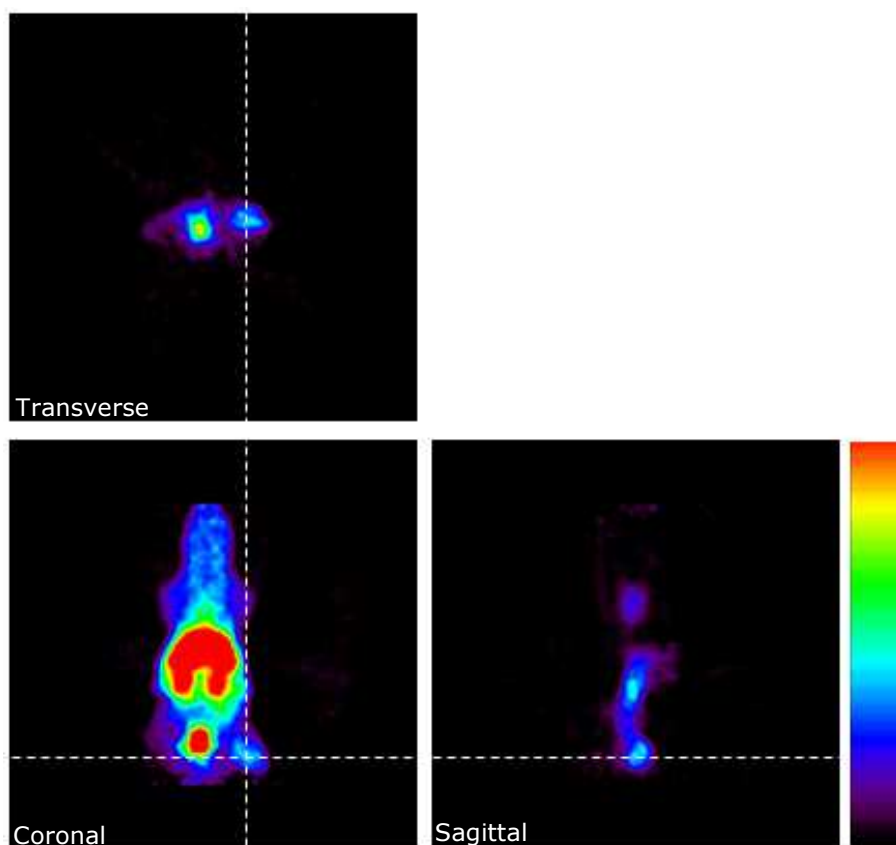


**Figure 11. Immuno-PET images of A549 tumor-bearing mice taken at 1 hr post injection of  $^{68}\text{Ga}$ -NOTA-Cetuximab Fab fragments.**

$^{68}\text{Ga}$ -NOTA-Cetuximab Fab fragments were intravenously administered to nude mice bearing A549 tumors. Immuno-PEG images were acquired at 1 hr post injection after anesthetizing the mice with 2% isoflurane.

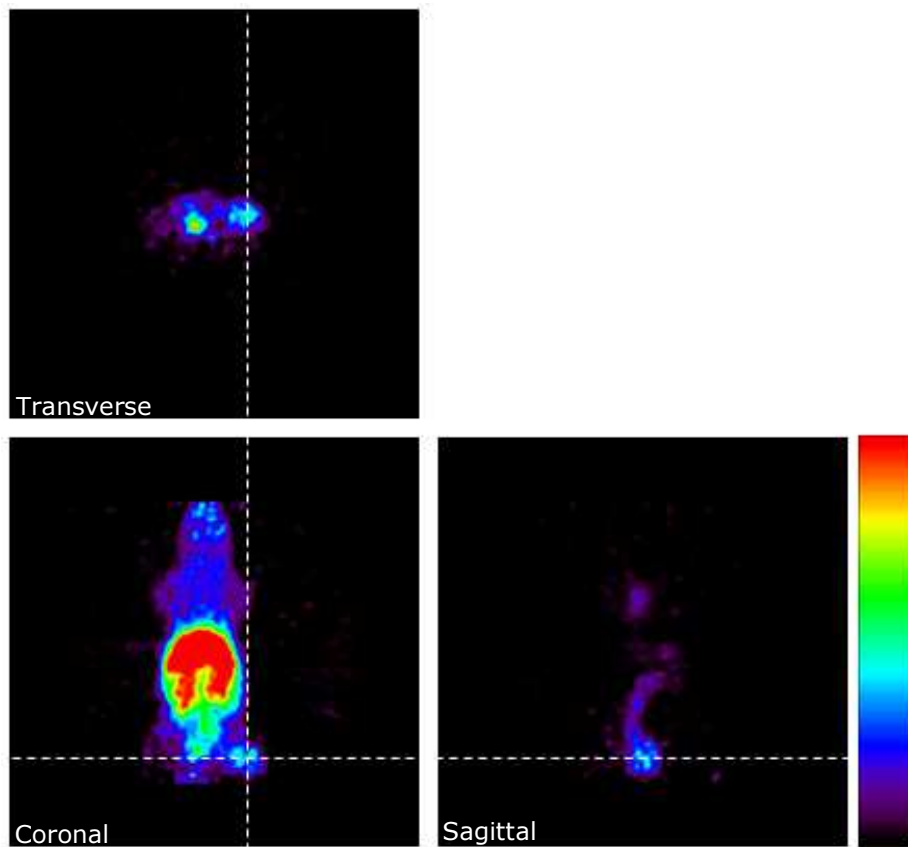


**Figure 12. Immuno-PET images of A549 tumor-bearing mice taken at 3 hr post injection of  $^{68}\text{Ga}$ -NOTA-Cetuximab Fab fragments.**

$^{68}\text{Ga}$ -NOTA-Cetuximab Fab fragments were intravenously administered to nude mice bearing A549 tumors. Immuno-PET images were acquired at 3 hr post injection after anesthetizing the mice with 2% isoflurane.

## IV. DISCUSSION

The purpose of this study was to develop immuno-PET imaging agents targeted to the EGFR over-expressing cancer. The Cetuximab, as an anti-EGFR mAb, was used by many researchers using the immuno-PET. The affinity of Cetuximab with the EGFR expressing cells and cancer was described [34-36]. Furthermore, the Fab fragments of the antibody have some advantages. The Fab fragments have an affinity to the target, and its blood clearance is faster than whole antibody [37-38]. Based on these consideration, in this study Cetuximab Fab fragments were adopted as a targeting ligand for the EGFR-expressing cancer. As described earlier  $^{68}\text{Ga}$  is a suitable radio isotope for the PET imaging because it has merits as a positron emitter such as  $^{18}\text{F}$ ,  $^{64}\text{Cu}$ ,  $^{124}\text{I}$ , and other things.

The immunoreactivity of Cetuximab Fab fragments was maintained approximately 55% of whole IgG molecule of Cetuximab at the same molar amount. In general, the conjugation of chelating agent influence on the affinity of the igG or its derivatives. Interestingly, however, NOTA conjugation to the Fab fragment did not interfered with its immunoreactivity. The immunoreactivity of  $^{68}\text{Ga}$ -NOTA-Cetuximab Fab fragments were very similar to that of  $^{125}\text{I}$ -Cetuximab Fab fragments. Simply use of the  $^{68}\text{Ge}/^{68}\text{Ga}$  generator was established by many times of elution over the course of this study. The  $^{68}\text{Ga}$ -radiolabeling to the Fab fragments was convenient at a high yield. In addition, the radiolabeled Fab fragments were very stable in a high concentration of serum proteins. The structural stability in the blood circulation system is

another prerequisite for a PET imaging agent.

The intravenously administered  $^{68}\text{Ga}$ -Cetuximab Fab fragments appeared to be specifically localized in the A549 tumor xenograft in mice even though they were primarily accumulated in the liver, kidneys, and bladder. The liver belongs to the blood pool and accumulation in the kidneys implies excretion of Fab fragments from the body. Meanwhile, the biodistribution studies in mice carry the A549 tumors exhibited a relatively lower accumulation of Cetuximab radiolabeled with  $^{126}\text{I}$  or  $^{68}\text{Ga}$  in the tumor tissues. This inconsistent patterns of intratumoral localization from the immuno-PET imaging and biodistribution assay need to be clarified by further investigation. Previous studies have shown that the  $^{68}\text{Ga}$ -NOTA-conjugated peptides or proteins are primarily accumulated in the liver, kidneys and tumor tissues [23-25]. It has also reported that Fab fragments more rapidly cleared through the kidneys than the whole IgG molecules [27-28]. Therefore, it can not be yet concluded whether the higher accumulation of  $^{68}\text{Ga}$ -Cetuximab Fab fragments in tumor tissues is mediated by their specific recognition of tumors.

At present, the cancer diagnosis is routinely done by X-ray, cytologic examination of biopsies, quantification of tumor antigens in serum test and so on. Recently, a great deal of effort has been spent to develop immuno-PET imaging adopting tumor-specific antibodies and positron emitters for clinical cancer diagnosis. Like other immuno-PET systems, the  $^{68}\text{Ga}$ -Cetuximab Fab fragments would be an efficient, harmless, rapid and non-invasive method of diagnosis for the EGFR over-expressing cancers. According to the experimental results of this research, the  $^{68}\text{Ga}$ -NOTA-Cetuximab Fab fragments can be utilized as an effective PET imaging agent for diagnosis of EGFR over-expressing cancers.

## VI. REFERENCE

1. Klapper LN, Kirschbaum MH, Sela M, Yarden Y. Biochemical and clinical implications of the ErbB/HER signaling network of growth factor receptors. *Adv Cancer Res* 2000;77:25-79
2. Baselga J. The EGFR as a target for anticancer therapy-focus on Cetuximab. *Eur J Cancer* 2001;37:S16-S22
3. Rossi A, Maione P, Gridelli C. Cetuximab in advanced non-small cell lung cancer. *Cri Rev Onc Hem* 2006;59:139-149
4. Salomon DS, Brandt R, Ciardiello F, Normanno N. Epidermal growth factor-related peptides and their receptors in human malignancies. *Cri Rev Onc Hem* 1995;19:183-232
5. Rivera F, Vega-villegas ME, Lopez-Brea MF. Cetuximab, its clinical use and future perspectives. *Anti-Cancer Drugs* 2008;19:99-113
6. Mendelsohn J, Baselga J. Status of Epidermal Growth Factor Receptor Antagonists in the Biology and Treatment of Cancer. *J Clin Oncol* 2003;21:2787-2799
7. Humblet Y. Cetuximab: and IgG1 monoclonal antibody for the treatment of epidermal growth factor receptor-expressing tumours. *Expert Opin*

*Pharmacother* 2004;5:1621-33

8. Baselga J, Canadas M, Codony J, Hueto J, Arcas A, Llado A, Puig X, Guix M, Raspall G, Albanell J. Activated epidermal growth factor receptor: studies in head and neck tumors and tumor cell lines after exposure to ligand and receptor tyrosine kinase inhibitors. *Proc Am Soc Clin Oncol* 1999;18:2392
9. Waksal HW. Role of an anti-epidermal growth factor receptor in treating cancer. *Cancer Meta Rev* 1999;18:427-436
10. van Dongen GAMS, Visser GW M, Lub-de Hooge MN, De Vries WG, Perk LR. Immuno-PET: A Navigator in Monoclonal Antibody Development and Applications. *Oncologist* 2007;12:1379-1389
11. McBride WJ, Zanzonico P, Sharkey RM, Noren C, Karacay H, Rossi EA, Lsman MJ, Brard PY, Chang CH, Larson SM, Goldenberg DM. Bispecific Antibody Pretargeting PET(ImmunoPET) with an <sup>124</sup>I-Labeled Hapten-Peptide. *J Nucl Med* 2006;47:1678-1688
12. Verel I, Visser GWM, van Dongen GA. The Promise of Immuno-PET in Radioimmunotherapy. *J Nucl Med* 2005;46:164S-171S
13. Saleem A, Charnley N, Price P. Clinical molecular imaging with positron emission tomography. *Euro J Cancer* 2006;42:1720-1727

14. Wu AM, Williams LE, Zieran L, Padma A, Sherman MA, Bebb GG, Odom-Maryon T, Wong JYC, Shively JE. Anti-Carcinoembryonic antigen (CEA) diabody for rapid tumor targeting and imaging. *Tumor Targeting* 1999;4:47-58
15. Cutler CS, Wuest M, Anderson CJ, Reichert DE, Sun Y, Martell AE, Welch MJ. Labeling and in vivo evaluation of nobel copper(II) Dioxotetraazamacrocyclic complexes. *Nucl Med Bio* 2000;27:375-380
16. Cole WC, DeNardo SJ, Meares CF, McCall MJ, DeNardo GL, Epstein AL, O'Brien HA, Moi MK. Comparative serum stability of radiochelates for antibody radiopharmaceuticals. *J Nucl Med* 1987;28:83-90
17. Moi MK, Meares CF, McCall MJ, Cole WC, DeNardo SJ. Copper chelates as probes of biological systems: Stable copper complexes with a macrocyclic bifunctional chelating agent. *Anal Biochem* 1985;148:249-253
18. Jones WTM, Deal KA, Anderson CJ, McCarthy DW, Kovacs Z, Motekaitis RJ, Sherry AD, Martell AE, Welch MJ. The in vivo behavior of copper-64-labeled azamacrocyclic compounds. *Nucl Med Biol* 1998;25:523-530
19. Breeman WA, Verbruggen AM. The  $^{68}\text{Ge}/^{68}\text{Ga}$  generator has high potential, but when can we use  $^{68}\text{Ga}$ -labelled tracers in clinical routine? *Eur J Nucl Med Mol Imaging* 2007;34:978-981

20. Ehrhardt GJ, Welch MJ. A new Germanium-68/gallium-68 generator. *J Nucl Med* 1978;19:925-929.
21. Schumacher J, Maier-Borst W. A new <sup>68</sup>Ge/<sup>68</sup>Ga radioisotope generator system for production of <sup>68</sup>Ga in dilute HCl. *Int J Appl Radiat Isot* 1981;32:31-36
22. Ambe S. <sup>68</sup>Ge/<sup>68</sup>Ga generator with alpha-ferric oxide support. *Appl Radiat Isot* 1988;39:49-51
23. Griffiths GL, Chang CH, McBride WJ, Rossi EA, Sheerin A, Tejada GR, Karacay H, Sharkey RM, Horak ID, Hansen HJ, Goldenberg DM. Reagents and methods for PET using bispecific antibody pretargeting and <sup>68</sup>Ga-radiolabeled bivalent hapten-peptide-chelate conjugates. *J Nucl Med* 2004;45:30-39
24. Velikyan I, Beyer GJ, Bergstrom-Pettermann E, Johansen P, Bergstrom M, Langstrom B. The importance of high specific radioactivity in the performance of <sup>68</sup>Ga-labeled peptide. *Nucl Med Bio* 2008;35:529-536
25. Jeong JM, Hong MK, Chang YS, Lee YS, Kim YJ, Cheon GJ, Lee DS, Chung JK, Lee MC. Preparation of a promising angiogenesis PET imaging agent: <sup>68</sup>Ga-labeled c(RGDyK)-isothiocyanatobenzyl-1,4,7-triazacyclononane-1,4,7-Triacetic acid and feasibility studies in mice. *J Nucl Med* 2008;49:830-836

26. Mirzadeh S, KNAPP FF. Biomedical radioisotope generator systems. *J Radioanalytical Nucl Chem* 1996;203(2):471-488
27. Lu SX, Takach EJ, Solomon M, Qing Z, Law SJ, Hsieh FY. Mass Spectral analyses of labile DOTA-NHS and heterogeneity determination of DOTA or DM1 conjugated anti-PSMA antibody for prostate cancer therapy. *J Pharm Sci* 2005;94(4):788-797
28. Hofmann M, Maecke H, Borner AR, Weckesser E, Schoffski P, Oei L, Schumacher J, Henze M, Heppeler A, Meyer J, Knapp H. Biokinetics and imaging with the somatostatin receptor PET radioligand <sup>68</sup>Ga-DOTATOC: preliminary data. *Eur J Nucl Med* 2001;28:1751-1757
29. Parker D. Tumor targeting with radiolabeled macrocycle-antibody conjugates. *Chem Soc Rev* 1990;19:271-291
30. Cox JPL, Craig AS, Helps IM. Synthesis of C- and N-functionalized derivatives of 1,4,7-triazacyclononane-1,4,7-triacetic acid (NOTA), 1,4,7,10-tetraazacyclododecane-1,4,7,10-tetraacetic acid (DOTA), and diethylenetriaminepentaacetic acid (DTPA): bifunctional complexing agents for the derivatization of antibodies. *J Chem Soc Perkin Trans* 1990;1:1567-1576
31. Studer M, Meares CF. Synthesis of novel 1,4,7-triazacyclononane-N,N',N''-triacetic acid derivatives suitable for protein labeling. *Bioconjug Chem* 1992;3:337-341

32. McMurry TJ, Brechbiel M, Wu C, Gansow OA. Synthesis of 2-(p-thiocyanato-benzyl)-1,4,7-triazacyclononane-1,4,7-triacetic acid: application of the 4-methoxy-2,3,6-trimethylbenzenesulfonamide protecting group in the synthesis of macrocyclic polyamines. *Bioconjug Chem* 1993;4:236-245
33. Brechbiel MW, McMurry TJ, Gansow OA. A direct synthesis of a bifunctional chelating agent for radiolabeling proteins. *Tetrahedron Lett* 1993;34:3691-3694
34. Perk LR, Visser GW, Vosjan MJ, Stigter-van WM, Tijink BM, Leemans CR, van Dongen GA. (89)Zr as a PET surrogate radioisotope for scouting biodistribution of the therapeutic radiometals (90)Y and (177)Lu in tumor-bearing nude mice after coupling to the internalizing antibody cetuximab. *J Nucl Med* 2005;46(11):1898-906
35. Cai W, Chen K, He L, Cao Q, Koong A, Chen X. Quantitative PET of EGFR expression in xenograft-bearing mice using <sup>64</sup>Cu-labeled cetuximab, a chimeric anti-EGFR monoclonal antibody. *Eur J Nucl Med Mol Imaging* 2007;34(6):850-8
36. Di Fabio F, Pinto C, Rojas Llimpe FL, Fanti S, Castellucci P, Longobardi C, Mutri V, Funaioli C, Sperandi F, Giaquinta S, Martoni AA. The predictive value of <sup>18</sup>F-FDG-PET early evaluation in patients with metastatic gastric adenocarcinoma treated with chemotherapy plus cetuximab. *Gastric Cancer* 2007;10(4):221-7

37. Covell DG, Barbet J, Holton OD, Black CDV, Parker RJ, Weinstein JN. Pharmacokinetics of monoclonal immunoglobulin G<sub>1</sub>, F(ab')<sub>2</sub>, and Fab' in Mice. *Cancer Res* 1986;46:3969-78

38. Fujimori K, Covell DG, Fletcher JE, Weinstein JN. Modeling analysis of the global and microscopic distribution of immunoglobulin G, F(ab')<sub>2</sub> and Fab in Tumors. *Cancer Res* 1989;49:5656-63

## 국문 요약

# **$^{68}\text{Ga}$ -NOTA-Cetuximab Fab을 이용한 EGFR 과발현 종양 이식 모델의 소동물 PET영상 및 생체 분포**

연세대학교 대학원

임상병리학과

김도완

Cetuximab (C225, anti-EGFR mAb)은 epidermal growth factor receptor (EGFR)에 특이적으로 결합하는 152 kDa의 키메라 항체이며, EGFR은 세포막 단백질로서, 세포의 분열 증식에 관여하는데, 이는 다양한 고형 암세포에서 과발현 한다고 알려져 있다. 현재 암의 진단에 immuno-PET (Positron Emission Tomography)의 중요성이 증대되고 있으며, PET 영상에 표적자로 쓰일 수 있는 Gallium-68 ( $^{68}\text{Ga}$ )의 장점 또한 커지고 있다. 왜냐하면,  $^{68}\text{Ga}$ 의 반감기는 67.6분으로 양전자를 방출하는 방사성동위원소이며,  $^{68}\text{Germanium}/^{68}\text{Ga}$  generator에서 생산 되어 사용의 편리함 또한 갖고 있기 때문이다. 이번 연구에서는 Cetuximab의 Fab 절편에 NOTA를 결합 시키고  $^{68}\text{Ga}$ 을 표지하였으며, 이 표지물을 이용하여 immuno-PET 영상으로 EGFR 과발현 암을 이식한 동물 모델에서의 암 진단 여부를 확인 하였다.

Cetuximab의 Fab 절편은 papain 효소 처리를 하여 생산하였고, 생산한 Cetuximab Fab 절편은 12% acrylamide gel 상에서 순도를 확인 하여 연구에 이용하였다. 본 연구에 사용된 세포주 들의 EGFR 발현 정도를 확인하기 위하여 RT-PCR 분석과 Western blotting, immuno-chemistry 시험을 하여 A549 세포주에서 EGFR mRNA와 EGFR의 발현을 확인 할 수 있었다. Cetuximab Fab 절편에  $^{68}\text{Ga}$ 을 표지 하기 위하여 1,4,7-triazacyclononane-1,4,7-triacetic acid (NOTA)를 결합 시켰다. NOTA를 결합시킨 Cetuximab Fab 절편의 면역 반응성을 확인하기 위하여 세포 결합능 시험을 실시 하였 으며, NOTA를 결합시킨 Cetuximab Fab 절편의 면역 반응성은, 같은 몰수의 Cetuximab에 비하여 약 55%의 결합능을 보였다.  $^{68}\text{Ga}$ -NOTA-Cetuximab Fab 절편의 방사표지율은 Instant thin layer chromatography (ITLC)로 확인하여 95% 이상으로 동물 실험에 바로 이용할 수 있었다. 만들어진  $^{68}\text{Ga}$ -NOTA-Cetuximab Fab 절편으로 피하에 암세포 (A549)를 이식한 동물 모델에서 생체 장기 분포 실험을 실시하고, 소동물 PET 영상을 획득 하였다. 생체 장기 분포 실험과, PET 영상 결과 이식한 부위의 암 (A549)과 신장, 간의 집적을 확인 하였다.

본 연구에서 생산한  $^{68}\text{Ga}$ -NOTA-Cetuximab Fab 절편은  $^{68}\text{Ga}$ 의 짧은 반감기와 Fab 절편의 빠른 체외 배출로 인하여 방사선에 의한 피해가 적고 비침습적인 EGFR 과발현 암 진단제로서의 가능성을 확인 하였다.

---

핵심어 : EGFR, Cetuximab,  $^{68}\text{Ga}$ , NOTA, Fab